A MEMS Sensor for Gas Detection in High Voltage Oil Filled Equipment

Krishna Prasad Bhat, *Student Member IEEE,* Kwang W. Oh, *Member IEEE,* Douglas C. Hopkins, *Sr. Member IEEE*
Department of Electrical Engineering, State University of New York at Buffalo
D.Hopkins@IEEE.Org

***Abstract* - This paper addresses protection of oil insulated power equipment, e.g. transformers, using a MEMS sensor system to augment or replace existing protection techniques. Traditional technologies used for protection and analysis involve pressure and temperature sensing, gas chromatography and/or a Buchholz relay. A MEMS sensor is described to augment or replace such sensors. The proposed device is immersed within the insulating fluid, e.g. oil, and primarily consists of multiple micro scale turbines centrally shafted to a MEMS generator. The device utilizes relative differences in velocity, pressure and flow rate, of gas emanating from stressed or degrading insulation. A differential electrical output is produced which can be RF or photon coupled to a user interface.**

I. INTRODUCTION

An oil-filled power transformer is used as a case study to develop a MEMS-based gas sensor approach for high voltage apparatus. Oil inside a transformer undergoes relatively rapid decomposition depending on the type of fault or overload conditions [1]. The decomposition generates small amounts of gas molecules at high velocities and at relatively higher pressure and temperature than the surrounding oil [2]. The energy stored within the gas molecules can be compared to that of the surrounding oil as a function of quantity and time, and then converted to a variable electrical output by using a MEMS sensor consisting of multiple micro turbines centrally shafted to a micro generator. The turbine generator model is setup within a silicon dioxide encapsulated structure to be placed deep within the oil at close proximities to the transformer windings. Using multiple MEMS sensors within the transformer, it is possible to create a three dimensional image of the transformer, analyzing individual spots for degrading insulation and overload conditions depending on the amount of gas produced and oil displaced. The voltage outputs of the MEMS generators are transmitted through RF or photonic means to an external receiving unit, which aggregates the multiple sensor data for spatial mapping.

II. GAS PRODUCTION

The gas is primarily produced by the chemical and physical decomposition from high voltage gradients across the windings or from winding vibrations. The quantity of gas produced can vary anywhere from a cubic centimeter to 2 m^3 [3]. Almost 70% of the gas generated during normal and a fault condition is comprised of Hydrogen [4]-[9]. During extreme faults, the overall oil displacement reaches up to 5 m/s and the corresponding volume of gas due to vaporization could reach up to 3.4m^3. For the MEMS sensor, the areas of interest are low intensity faults, ~2kJ followed by a pressure wave of ~100kPa, and normal operating energy levels in the range of nJ to μJ. It has been shown that during a fault of energy 2kJ, there is substantial gas production (Hydrogen and Acetylene). The corresponding velocity of the gas bubbles can range between 0.1 – 0.5 m/s during minor fault conditions depending on the type of oil and transformer in use [3]. The amount of gas produced drastically increases the risk of a transformer explosion. For the very low intensity operation, it has been shown that, in certain insulating liquids, localized injection of electrical energy (1-20nJ) creates gas bubbles (~μm) followed by a low-pressure wave [10]. The Rayleigh Model relates the bubble lifetime (Δt) to the maximum bubble radius (R_m), density (ρ) and hydrostatic pressure (P) as shown in (1).

$$\Delta t = 1.83 R_m \sqrt{\frac{\rho}{P}}. \qquad (1)$$

The bubble radius can be related to the injected energy (E) and Boltzmann Constant (k) using a similar thermodynamic model as shown in (2).

$$R_m = k \left(\frac{E}{P}\right)^{\frac{1}{3}} \qquad (2)$$

Equations (1) and (2) are used further in section III B. to relate gas bubble formation to the energy transfer.

III. CONSTRUCTIONAL DESIGN AND WORKING OF THE MEMS SENSOR

The positioning of the proposed MEMS sensor is shown in Fig 1. The sensor is physically attached at multiple positions around the transformer-winding stack to maximize oil and gas bubble flow through the sensor. The advantage of using a MEMS-based sensor is to provide miniature features allowing it to span only one to two windings and be mounted on the windings. This presents a

978-1-4244-6395-4/10/$26.00 ©2010 IEEE

relatively low field gradient in a very high voltage transformer. The MEMS casing material must have a low dielectric constant, and withstand high electrical and mechanical stresses. Both ceramic and silicon dioxide are commonly used in microelectronics for high voltage gradient insulation, and would be used in this application.

The sensor includes a collection tube as shown in Fig 2. The tube has a collection port of calculated size for gas entrance to provide a calibrated gas volume. The area of the port opening is dependent on fluid (oil) characteristics, and changes depending on product application. The tube narrows and optimally concentrates the flow volume entering the turbine chamber.

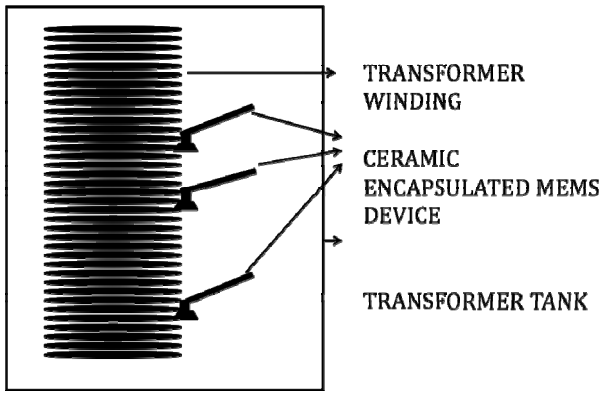

Fig 1. Positioning of MEMS device with span limited to few turns in transformer windings. Miniature size reduces field stress.

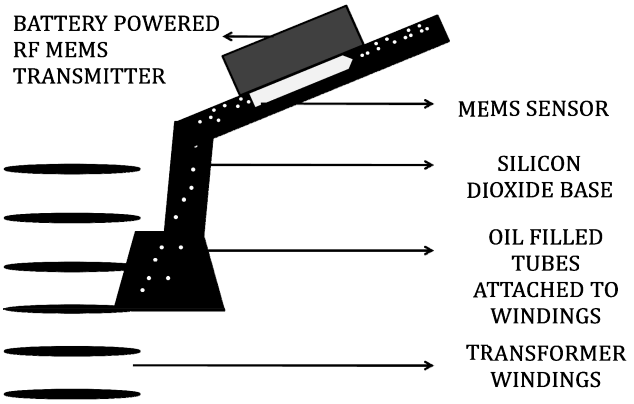

Fig 2. Shown is the conceptual design and positioning of MEMS components to form the MEMS transducer, along with a data transmitter.

A. MEMS Transducer – Turbine, Gearing and Generator

The MEMS transducer section of the sensor has four stages to transfer hydraulic energy into an electrical signal: graduated collection tube (noted above), MEMS turbine, gearing and generator. The MEMS turbine is the primary component of the transducer and transfers hydraulic energy of the bubble flow into rotational energy. Gearing is used to increase shaft speed, which in turn, drives a MEMS generator. The generator produces a proportional electrical output signal representing bubble generation by the stressed transformer windings. The arrangement of turbine and generator is shown in Figs. 3 and 4.

B. Working Principle

The turbine works on the principle that the gas bubble present in oil is at higher temperature, pressure and velocity than the surrounding oil [11]. Hence, the gas bubble has a relative difference in energy to the surrounding oil flow [12]. When the combined gas and oil flow impinges on the series of MEMS turbine blades, it converts some of its energy into mechanical rotation of the turbine. The MEMS device is used to measure the relative time difference in gas parameters during the various working conditions. During normal and fault conditions, the formation of bubbles can be explained as a fluidic interface given by the Young-LaPlace equation $\Delta P = \sigma \left(\frac{1}{R_1} + \frac{1}{R_2} \right)$ [13] where, ΔP is the difference in pressure between the enclosed gases and surrounding fluid, σ is the surface tension acting on the bubble and R_1, R_2 are the radii of curvature of the bubble [R_1, $R_2 < R_m$, from (1) and (2)].

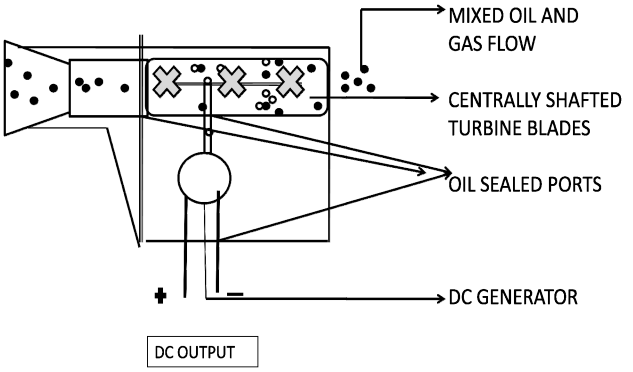

Fig 3. MEMS transducer placed within MEMS sensor. Gas flow enters a graduated collection tube and hydraulically drives at MEMS turbine. The turbine is geared to a generator, which produces an electrical signal proportional to gas flow.

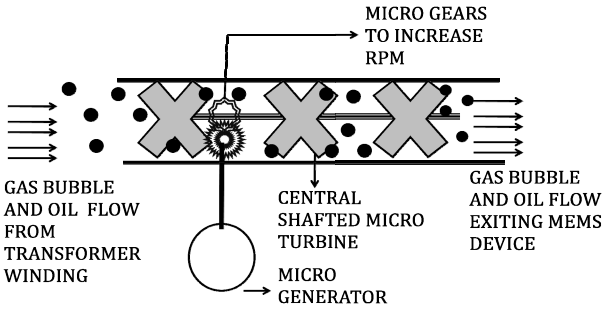

Fig. 4 - MEMS turbine and generator arrangement

Studies and experiments have shown that it is difficult to obtain a generalized equation for the exact velocity and energy enclosed by a gas bubble [12]. The energy depends on various factors: bubble formation, physical and

chemical properties of surrounding fluid, characteristic flow at the fluid interface, net forces acting on the oil – gas interface etc. However, the minimum work required to form a nucleus of gas [12] within a homogeneous liquid can be determined and used as a minimum design point. The work is given by

$$\Delta\Phi = \frac{4}{3}\pi R^3 \left[P_O - P + P\ln\frac{P}{P^*} \right] + 4\pi R^2\sigma + KT \sum_i n_i \ln\frac{y_i}{y_i^*} \quad (3)$$

where $\Delta\Phi$ = Minimum work done
P_o = Ambient (Nucleation) Pressure
P = Pressure of gas bubble
R = radius of gas bubble
K= Boltzmann constant
σ = Surface Tension of fluid interface.
n_i = Number of molecules of component in a Vapor mixture
y/y_i = Volume fraction

The closest approximation for the total energy of a gas bubble flowing through a fluid can be compared to the energy involved in the fluid layer interface (oil-gas) as shown in (4) [12].

$$dE = dE_1 + dE_2 + dE_3$$

$$E = \int_0^x \frac{\phi}{1-\phi}\rho_f g x Q_g + \rho_g + \frac{\rho_f}{2}\frac{v_f^2}{2\phi} + \frac{3\sigma}{R}\phi \, dx \quad (4)$$

where dE = Total energy of the layer
dE_1 = Potential energy of the gas
dE_2 = The kinetic energy of the layer
dE_3 = The energy due to surface tension
φ = Gas volume fraction
Q_g = Volumetric flow rate of gas
ρ_f = Density of fluid
ρ_g = Density of gas
v_f= Velocity of fluid interface
σ = Surface tension of fluid interface
x = Distance travelled by the interface
R = Radius of gas bubble

The exchange of energy at the intermolecular level and within the defined space, satisfies the energy conservation equations, such as mass, momentum and energy, as shown in (5) –(7) [14]. However, there is always a factor of loss in the practical process, which is mainly due to radiation following the transfer of energy from winding (electrical) to surrounding oil and its subsequent vaporization (mechanical). This loss is usually represented as a percentage depending on the type of fluid and the required form of energy, and is usually within 10 - 70% of the total electrical energy.

$$\frac{\partial\rho}{\partial t} + \frac{\partial\left(\rho\bar{c}_j\right)}{\partial x_j} = 0 \quad (5)$$

$$\frac{\partial\left(\rho\bar{c}_i\right)}{\partial t} + \frac{\partial\left(\rho\bar{c}_i\bar{c}_j\right)}{\partial t} = -\frac{\partial\rho}{\partial x_i} + \frac{\partial\tau_{i_j}}{\partial t} + \rho\overline{F_i} \quad (6)$$

$$\frac{\partial\left(\rho e + \frac{1}{2}\rho\bar{c}^2\right)}{\partial t} + \frac{\partial\left[\rho\bar{c}_j\left(h + \frac{1}{2}\bar{c}^2\right)\right]}{\partial t} = \frac{\partial\left(\tau_{jk} - q_i\right)}{\partial x_j} + \rho\overline{F}_j\bar{c}_j \quad (7)$$

where ρ = Density of gas.
c_{ij} = Molecular velocity vectors
F_i = Force per unit mass
τ = Energy flux
q_i = Heat flux
h = Enthalpy
e = Energy per unit mass

The energy transfer from the windings to the oil is given by $\acute{E} = W \times H(t)$ [3], where $\acute{E}$ is a percentage of the total energy (E) and W is the instantaneous power.

The combined mechanical output power of the micro-turbine (percentage of W) following the transfer of energy from the gas bubble and oil flow, is given by Von Karman's equation [15]

$$P = 2M\omega$$

$$M = 0.31\pi\rho a^4\sqrt{\nu\omega^3} \quad (8)$$

where P = Power output
M = Torque developed

Equation (8) indicates that the power developed by the rotor depends proportionally on both the kinematic viscosity of the fluid and the angular velocity of the turbine blade. However, in actuality, the angular velocity of the blade is inversely proportional to the kinematic viscosity as indicated by Newtonian flow equation $\tau = \nu\rho\partial x/\partial t$ where τ is the stress acting on the fluid, υ and ρ are the respective dynamic viscosity and density of oil. As seen from the expression, for a constant stress, higher the viscosity lower is the velocity. This reflects on (8) under which, the power developed can be expressed as a function $f = \left\{\omega^{5/2}\left(\nu^{-1}\right)\nu^{1/2}\right\}$ The final design characteristics of the sensor are dependent on the energy transfer efficiency of the gas bubble. This is dependent on many factors specific to applications and requires a computational approach evaluating specifics of the well-understood transfer mechanism [12].

IV. Reverse Scaling

The working of a micro pump can be closely related to the reverse working of a MEMS transducer. Micro rotary pumps, such as shown in Fig 5, with diameters of 2.3 mm have been designed for pumping fluids at the rate of 2.1 ml/min, achieved at a pressure of 1.19 kPa and 211 rpm [16]. An equivalent reverse function of the pump with relevant or reduced design parameters can produce electrical signals within a relative range needed for this application. The construction of a micro generator varies from that of a micro pump with appropriate changes to the turbine blade design and channeling of fluid flow. With the present limited options to show an actual design of a fluidic turbine geared specifically for power generation, it is necessary to relate design changes to existing micro pumps. Further research and demonstration would optimize design of impeller blades and flow interface to optimize mechanical power generation.

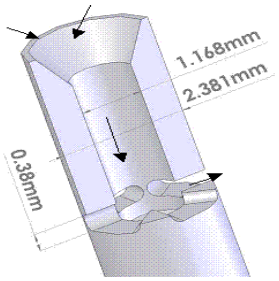

Fig 5. Double Disk Viscous Micro-Pump Developed at the University at Utah, Mechanical Engineering, March 2005 [16]

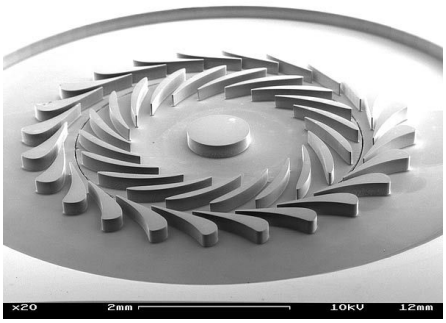

Fig 6. Shown is a 4mm rotor dia radial flow turbine used for power generation through Hydrogen combustion. Designed by Gas Turbine Laboratory, MIT Cambridge 2003. [16]

Combustion turbines exist for power generation. One such turbine shown in Fig 6 is used for power generation through micro (μm) rotary components and demonstrates the feature sizes required for the MEMS transducer. As explained in section III, the MEMS sensor attached to the transformer windings is used to collect the combined flow of gas and oil during the degradation of insulation. The size of the bubble and the duration for which it maintains its physical size and shape is primarily explained by (1) and (2). The energy from the transformer windings is used to form gas bubbles as mentioned by (3). As indicated, the size, time and energy of the gas bubble are interrelated and directly proportional to the energy generated by the winding during abnormal conditions. The oil and gas close to the winding are at a relatively higher energy, as represented in (4). The fluid flow then carries the mass, energy and momentum (specific to (5)-(7)) over a distance for the specific duration of time (Δt), dependent on the type, time period and intensity of transferred energy. Equations (1) through (7) provide the design requirements for feature size of the impellers and desired rotational speed. Further, the series turbine arrangement (Fig 4) optimizes energy transfer and uses a lower rpm.

The authors of [16] (Fig. 5) report a pumping capacity of 2.1 ml/min with head pressure of 1.19 kPa at 211 rpm. From the discussion in Section II, the overall gas flow available to the MEMS sensor can be up to 0.5 m/s. For a 3 mm effective radius impeller, this translates to 43 rpm, and would be accompanied with a pressure wave up to 100 kPa during abnormal transformer fault operation. The feature dimensions cited here for MEMS devices are within the range needed to produce the proposed MEMS sensor

A centrally shafted micro generator is used to produce an electrical signal proportional to gas flow. The micro generators are normally designed to operate at relatively higher rpm (>1000 rpm). Some of the present manufactured gears and low power permanent magnet generators are shown in Fig 7 & 8. The micro gear and generator set are isolated from the oil flow.

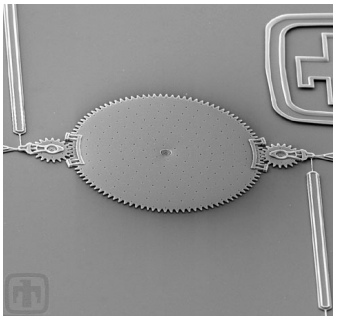

Fig 7. Shown is micro gearing demonstrated by Sandia National Laboratories, Sandia ST&E Micro Systems & Gears. [18]

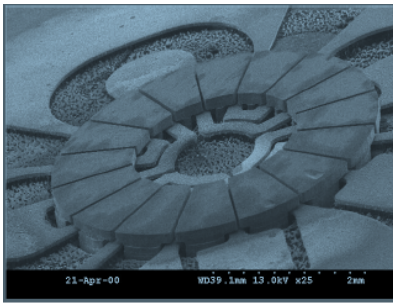

Fig 8. Shown is a 4mm dia. Magnetic Motor/Generator used in the MIT Gas Turbine project. [16]

V. Design Summary

Sustained transfer of energy is the critical step in the sensing of abnormal changes in the transformer. The close proximity of the sensor to the winding, improves the possibility for the fluid (gas & oil) to pass through the sensor. With the large volume of fluid (as compared to the size of turbine) passing through the sensor, the energy and momentum are transferred to the fluid turbine blades. The blades are the most important component of the sensor and are optimally designed to operate at low energy levels and rpm. Further, the turbine blade design should be specific to the application. For example, power transformers >200MVA operate at very high potentials and the possible transfer of energy during abnormal conditions can be higher than that compared to that of a lower power pole transformers. Therefore, the turbine design of a MEMS sensor, used in a power transformer can be relatively larger in size to match the magnitude of energy transferred.

The generator design follows a similar rule to that of the turbine. However, the manufacturing process can be more streamlined by using permanent magnet DC motors/generator set. This helps in providing a quick response output to the turbine torque and also eliminates field currents. The size of the generator would directly correspond to that of the turbine owing to the transfer of energy from the winding.

The output of the generator is then fed to an RF MEMS transmitter, which produces an RF signal in direct relation to that of the electrical DC output. The advantage of selecting the RF is the uniformity of oil as a transmission medium. Alternatively, a photonic link can be use to pass optical signals to a centralized collection point. Though optical fiber may be more impractical during maintenance operations. Similar to the selection of electro-mechanical components for the RF device, the designated RF transmission frequency of a MEMS sensor has to be selected considering the RF interference from partial discharge and high voltage transients.

VI. Summary

The present protection techniques in high voltage power apparatus using standard chemical, pressure, or temperature analysis can be augmented or replaced by the addition of a proposed MEMS sensor. The micro-size and high-volume production of MEMS devices provides greater flexibility in applications of sensing as compared to existing techniques. Sensing of multiple positions within a high voltage structure, such as a high voltage power transformer, can be analyzed to create a three dimensional image of the apparatus performance. However, the specific design of a MEMS sensor for installation inside oil filled equipment requires tailored practical testing and an applications oriented simulation tool.

VII. References

[1] Yong Chun Liang, Jian Le Liu "Power Transformer Based Diagnosis using SOM based RBF Neural Netwroks," Fifth Int'l. Conf. of Machine Learning and Cybernetics, Dalian, August 2006

[2] F. Jomni, F. Aitken and A. Denat "Investigation of the behaviour of Microscopic Bubbles in Insulating Liquids: Transition from Inertial Regime to the Viscous One," Proceedings of 14th Int'l. Conf. of Dielectric Liquids (ICDL 2002), Austria, 12 July 2002

[3] Sebastien Muller, Margareta Petrovan Boiarciuc and Guillaume Perigaud, "Protection of oil-filled Transformer against explosion: Numerical Simulations on a 200 MVA Transformer," 2009 IEEE Bucharest Power Tech Conf., June 28-July 2, Bucharest, Romania

[4] Zhang, Y, Ding, X, Liu, Y, Griffin, P. J., "An Artificial Neural Network Approach to Transformer Fault Diagnosis," IEEE Trans. on Power Delivery, Vol. 11, No. 4, p. 1836-1841 (1996).

[5] Guardado, J. L., Naredo, J. L., Moreno, P.; Fuerte, C. R. (2001). A Comparative Study of Neural Network Efficiency in Power Transformers Diagnosis Using Dissolved Gas Analysis. IEEE Trans. on Power Delivery. Vol. 16, No. 4, p. 643-647.

[6] Dukarm, J. J., "Transformer Oil Diagnosis Using Fuzzy Logic and Neural Networks," Conf. in Electrical and Computer Engineering, Canadian, Vol. 1, p. 329-332 (1993).

[7] Lin, C. E.; Ling, J. M. e Huang, C. L., An Expert System for Transformer Fault Diagnosis Using Dissolved Gas Analysis. IEEE Trans. on Power Delivery, Vol. 8, No. 1, p. 231-238 (1993)

[8] Xu, W., Wang, D., Zhou, Z. e Chen, H., "Fault Diagnosis of Power Transformers: Application of Fuzzy Set Theory, Expert Systems and Artificial Neural Networks," IEE Proc.-Sci. Meas. Technology, Vol.144, No. 1, p. 39-44 (1997).

[9] Huang, Y. C., Yang, H., T. Huang, C. L., "Developing a New Transformer Fault Diagnosis System through Evolutionary Fuzzy Logic," IEEE Trans. on Power Delivery, Vol. 12, No. 2, p 761-767

[10] F. Jomni, F. Aitken and A. Denat, "Dynamics of microscopic bubbles generated by a corona discharge in insulating liquids," *J. of Electrostatics*, Vol. 47, Issue 1-2, June 1999, p. 49-59.

[11] Sylvain Prigent, et.al, "Comparison of the SERGI Developed Magneto-Thermo-Hydrorynamic Model Results with Measurements Made on a 160KVA Transformer," IEEE Section Mexico, Acapulco, July 9 to 14, 2000, IEEE Ref: rpijp01a, dated 29/05/00

[12] N. P. Cheremisinoff, Ed., "Encyclopedia of Fluid Mechanics," Chap. :Gas-Liquid Flows," Vol. 3 *Lib. of Congress Cataloging-in-Publication Data*, Gulf Publishing Company, Houston, TX, p 130-140, 58, 341, 344, 142.

[13] John A. Pelesko, David H. Bernstein, "Modeling MEMS and NEMS," Chapman & Hall/CRC Press Company, Corporate Blvd. Boca Raton, Fl, pp76-77.

[14] Walter G. Vincenti, Charles H. Kruger, Jr., "*Intro to Physical Gas Dynamics*", John Wiley & Sons, Inc. NY, 1965, p 316-327.

[15] Jonathan Kao, et.al, "A bubble Powered Micro-rotor: Manufacturing, Assembly and Characterization," Proc. of 2006 ASME Int'l. Mechanical Engineering Congress and Exp., Chicago, Illinois, Nov 5-10, 2006, IMECE2006-14675

[16] Blanchard D., Ligrani P., Gale B. "Single-Disk and Double-Disk Viscous Micropumps," Sensors and Actuators A: Physical, Vol. 122, Issue 1, 29 July 2005, p 149-158

[17] Alan H. Epstein, "Millimeter-Scale, MEMS Gas Turbine Engines", Gas Turbine Laboratory Massachusetts Institute of Technilogy, Cambridge MA, proceedings of ASME Turbo Expo 2003, Power for Land, Sea, and Air; June 16-19, 2003, Atlanta Georgia.

[18] Jeffry J. Sniegowski, "Chemical-mechanical polishing: enhancing the manufacturability of MEMS", Intelligent Micromachines Department, Sandia National Laboratories, Albuquerque, NM.